

# Quantitative Reactivity Scales for Dynamic Covalent and Systems Chemistry

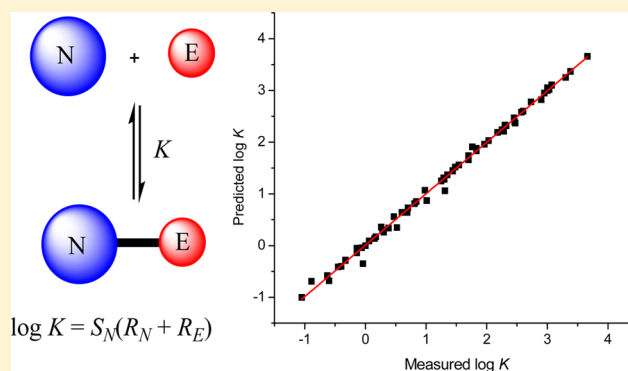
Yuntao Zhou,<sup>†,§</sup> Lijie Li,<sup>†,‡,§</sup> Hebo Ye,<sup>†,§</sup> Ling Zhang,<sup>†</sup> and Lei You<sup>\*,†</sup>

<sup>†</sup>State Key Laboratory of Structural Chemistry, Fujian Institute of Research on the Structure of Matter, Chinese Academy of Sciences, Fuzhou, Fujian 350002, PR China

<sup>‡</sup>University of Chinese Academy of Sciences, Beijing 100049, PR China

**S** Supporting Information

**ABSTRACT:** Dynamic covalent chemistry (DCC) has become a powerful tool for the creation of molecular assemblies and complex systems in chemistry and materials science. Herein we developed for the first time quantitative reactivity scales capable of correlation and prediction of the equilibrium of dynamic covalent reactions (DCRs). The reference reactions are based upon universal DCRs between imines, one of the most utilized structural motifs in DCC, and a series of O-, N-, and S-mononucleophiles. Aromatic imines derived from pyridine-2-carboxyaldehyde exhibit capability for controlling the equilibrium through distinct substituent effects. Electron-donating groups (EDGs) stabilize the imine through quinoidal resonance, while electron-withdrawing groups (EWGs) stabilize the adduct by enhancing intramolecular hydrogen bonding, resulting in curvature in Hammett analysis. Notably, unique nonlinearity induced by both EDGs and EWGs emerged in Hammett plot when cyclic secondary amines were used. This is the first time such a behavior is observed in a thermodynamically controlled system, to the best of our knowledge. Unified quantitative reactivity scales were proposed for DCC and defined by the correlation  $\log K = S_N(R_N + R_E)$ . Nucleophilicity parameters ( $R_N$  and  $S_N$ ) and electrophilicity parameters ( $R_E$ ) were then developed from DCRs discovered. Furthermore, the predictive power of those parameters was verified by successful correlation of other DCRs, validating our reactivity scales as a general and useful tool for the evaluation and modeling of DCRs. The reactivity parameters proposed here should be complementary to well-established kinetics based parameters and find applications in many aspects, such as DCR discovery, bioconjugation, and catalysis.



## INTRODUCTION

Dynamic covalent reactions (DCRs)<sup>1</sup> are being increasingly utilized for the construction and modulation of molecular assemblies, complex networks, as well as nanostructures,<sup>2</sup> which have found applications in sensing,<sup>3</sup> labeling,<sup>4</sup> catalysis,<sup>5</sup> and separation.<sup>6</sup> As a unique class of dynamic interactions, the interconversion through component exchange of DCRs under thermodynamic control can result in structural and functional diversity as well as complexity, which is central to the recently emerging field of systems chemistry.<sup>7</sup> For example, Sanders, Otto, and others built dynamic combinatorial libraries for the assembly and sorting of novel structures, such as interlocked molecules, which are challenging to make via traditional stepwise synthesis.<sup>8</sup> Nitschke, Leigh and others created cages, knots, helicates, and etc., by using the strategy of orthogonal assembly through imine formation and metal coordination.<sup>9</sup> On the basis of dynamic exchange of hydrazones, Kay achieved facile surface functionalization of gold nanoparticles.<sup>10</sup> Recently, Lehn developed a series of elegant dynamic covalent molecular walkers.<sup>11</sup> Covalent organic cages and porous frameworks have

also been designed for gas storage, such as those reported by Mastalerz and others.<sup>12</sup>

Despite tremendous advances have been made, one bottleneck in the field of dynamic covalent chemistry (DCC)<sup>1,13</sup> is that the scope of current DCRs is rather limited, with imine,<sup>14</sup> hydrazone,<sup>15</sup> disulfide,<sup>16</sup> and boronic ester<sup>17</sup> among the most exploited. As a result, there is continually growing interest in expanding the chemical space and thereby versatility of DCRs in order to gain access to new functions. For example, Zhang developed reversible alkene and alkyne metathesis and used them for cage construction.<sup>2b,18</sup> Taunton and Anslyn fine-tuned dynamic thio-Michael additions in aqueous solutions for reversible covalent labeling of cysteine.<sup>19</sup> Delius discovered a tripodal tool for DCC based on acid-catalyzed exchange reaction of orthoesters and constructed dynamic cryptates.<sup>20</sup> Other representative examples include dynamic enamines,<sup>21</sup> dynamic alkoxyamines,<sup>22</sup> diselenide exchange,<sup>23</sup> triazolinedione based reversible click chemistry,<sup>24</sup> and dynamic urea bond.<sup>25</sup> Instead of

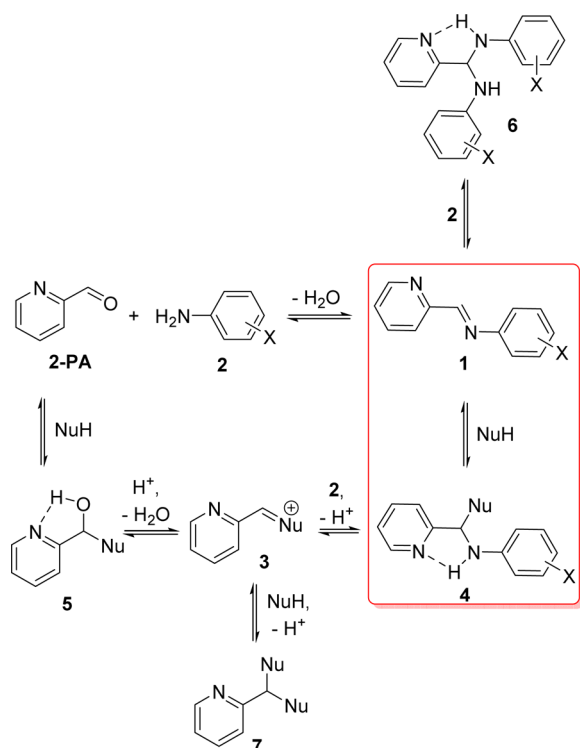
Received: October 30, 2015

Published: December 10, 2015

targeting specific functionality, recently we proposed a general concept of reactivity based dynamic covalent chemistry,<sup>26</sup> in which the term “reactivity” refers to the extent of the reaction a chemical species participates. The emphasis on reactivity in the field of DCC would unify various DCRs with different functionalities, and a corresponding quantitative scale with predictive power would be particularly useful for the discovery and manipulation of DCRs within the rich realm of equilibrium systems.

In order to establish reactivity scales for DCC, a set of reference DCRs with a wide range of equilibrium constants would be required. Imines are one class of the most utilized building blocks in supramolecular and systems chemistry.<sup>14</sup> Although their chemistry is highly diverse,<sup>27</sup> the reactivity of imines has rarely been exploited for DCR applications.<sup>28</sup> We envision that the electrophilicity of aromatic imines can be facilely modulated through substituent effect, and therefore, imines could serve as a versatile platform for the modeling of DCRs. Very recently, we reported the creation of amina based tri(2-picolyl)amine ligands using metal-templated dynamic multicomponent covalent assembly.<sup>28a</sup> Imines were found as the key intermediate, and the position of the equilibrium was modulated through substituent effect. In the current report, aromatic imines (**1**, Scheme 1) derived in situ from pyridine-2-

**Scheme 1. Equilibria and Intermediates for Imine Based DCRs**



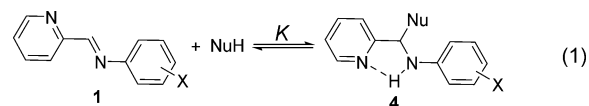
carboxyaldehyde (**2-PA**) were investigated systematically for reactivity based universal DCRs toward a series of mononucleophiles. Intrinsic resonance stabilization pattern in the reactant and product led to curvature in Hammett plots. In particular, unprecedented nonlinearity in Hammett plot was revealed for DCRs using cyclic secondary amines, with both electron-donating groups (EDGs) and electron-withdrawing groups (EWGs) significantly deviating from the line. Unified reactivity parameters were next developed for DCC using imine

based DCRs as references. The correlation of other DCRs was also accomplished, thereby validating the generality and predictive ability of our quantitative reactivity scales for DCC.

## RESULTS AND DISCUSSION

**Design.** Our primary focus is placed upon manipulating the reactivity of the imine as a means of harnessing the reversibility and stability. We postulated that the electrophilicity of aromatic imines derived from **2-PA** would be much higher than aliphatic imines due to electron-withdrawing nature of pyridine, and the reversible addition of O-, N-, S- nucleophiles is plausible. Instead of starting from preformed imines, dynamic multicomponent covalent assembly reactions were conducted with **2-PA**, primary aromatic amines (**2**), and mononucleophiles (NuH) in acetonitrile in order to control the equilibrium through in situ generated imines (Scheme 1). A competing pathway through oxonium like intermediate **3** via the direct addition of NuH to **2-PA** is possible depending on the relative nucleophilicity of **2** and NuH. However, we conceived that a delicate balance between the stability and reactivity of imine **1** could be established by fine-tuning through substitution on the aromatic ring.<sup>28a</sup> In addition to minimizing work of synthesis and isolation, such in situ assemblies would afford same extent of equilibrium irrespective of the sequence of reagent addition because the system is under thermodynamic control. Moreover, intramolecular hydrogen bonding could be used as a driving force to stabilize adduct **4**, thus providing a means for further modulating the equilibrium. In essence, we sought a general system that can reversibly bind a diverse set of mononucleophiles, which in turn could enable the creation of a library of DCRs with a wide range of equilibrium constants, thus laying the foundation for the establishment of quantitative scales for DCC.

**Deduction of Equilibrium Constant.** To quantify the DCR, equilibrium constant for the transformation of **1** to **4** (highlighted in Scheme 1) was derived. This two-component reaction directly correlates with the stability and reactivity of imine **1** (eq 1 and 2). All the concentrations can be deduced from



the total concentration of each reactant and the integrals in <sup>1</sup>H NMR spectra. By defining the integral ratio of **1** to **4** as *x*, the integral ratio of free **2-PA** to **4** as *y*, the integral ratio of free nucleophile to **4** as *z*, and the integral ratio of **2-PA** derived compounds except **1** and **4** (i.e., **5**, **6** and **7**) to **4** as *n*, the concentration of **4** is given in eq 3 according to the mass balance of **2-PA**. Substituting eq 3 into eq 2, combined with the defined ratios, affords the *K* expression for the assembly reaction (eq 4, see details in SI).

$$K = \frac{[\mathbf{4}]}{[\mathbf{1}][\text{NuH}]} \quad (2)$$

$$[\mathbf{4}] = \frac{[\mathbf{2-PA}]_{\text{total}}}{1 + x + y + n} \quad (3)$$

$$K = \frac{1 + x + y + n}{xz[\mathbf{2-PA}]_{\text{total}}} \quad (4)$$

**Optimization and Modulation of DCRs.** With the strategy in mind, the multicomponent reaction of **2-PA**, a primary

aromatic amine, and a model thiol (1-propanethiol) was screened. The reaction of 2-PA, 4-cyanoaniline, and thiol in acetonitrile afforded a mixture of aldehyde, product 4, as well as thiohemiacetal 5 after 24 h, with 2-PA being the major component, but no imine 1 was apparent (Figure S3 and Table S1). Surprisingly, the formation of 4 was almost quantitative when 0.3 equiv of methanesulfonic acid (MA) was present. The effect of acid is likely due to the acceleration of reactions through Brønsted acid catalysis. Assembly reactions were next performed with amine 2 of varied substitution in the presence of 0.3 equiv of MA individually, and the results are listed in Table 1. For all substituents tested, product 4 was the major

**Table 1. Component Distribution and Equilibrium Constants for Imine 1 Based DCRs with 1-Propanethiol**

X	2-PA (%)	1 (%)	4 (%)	K (M <sup>-1</sup> )
<i>p</i> -OCH <sub>3</sub> <sup>a</sup>	<1	30	69	22.2
<i>p</i> -CH <sub>3</sub> <sup>a</sup>	<1	11	89	90.4
<i>m</i> -CH <sub>3</sub> <sup>a</sup>	<1	6	93	176
<i>p</i> -H <sup>b</sup>	<1	26	73	296
<i>m</i> -F <sup>b</sup>	<1	16	83	1070
<i>m</i> -Br <sup>b</sup>	3	13	83	1170
<i>m</i> -CF <sub>3</sub> <sup>b</sup>	3	5	92	2000
<i>m</i> -CN <sup>b</sup>	4	7	89	2380
<i>p</i> -CN <sup>b</sup>	2	0	98	—
<i>p</i> -NO <sub>2</sub> <sup>b</sup>	2	0	98	—

<sup>a</sup>3.0 equiv of thiol. <sup>b</sup>1.0 equiv of thiol.

species. As the arene becomes more electron-deficient, the equilibrium constant increases with a range of 22.2–2380 M<sup>-1</sup>. The equilibrium constant was not obtained for 4-cyanoaniline and 4-nitroaniline because imine 1 was not detected.

For monoalcohols, ethanol was chosen as a model. Only trace amount (less than 2%) of hemiaminal ether 4 was detected when 4-nitroaniline was used (Figure S5 and Table S2). However, there was a significant increase (around 25%) in product 4 upon the addition of MA. The multicomponent reactions were then conducted with individual aniline derivative in the presence of 0.3 equiv of MA. Not surprisingly, only the imine incorporating EWGs afforded detectable amount of 4 in <sup>1</sup>HNMR, with a percentage range of 2–28% (Table 2). In all cases, both aldehyde

**Table 2. Component Distribution and Equilibrium Constants for Imine 1 Based DCRs with Ethanol<sup>a</sup>**

X	2-PA (%)	1 (%)	6 (%)	4 (%)	K (M <sup>-1</sup> )
<i>m</i> -Br	11	87	0	2	0.24
<i>m</i> -CF <sub>3</sub>	9	87	0	3	0.36
<i>m</i> -CN	13	83	0	4	0.47
<i>p</i> -CF <sub>3</sub>	18	75	0	7	1.00
<i>p</i> -CN	24	53	4	19	3.30
<i>p</i> -NO <sub>2</sub>	37	29	6	28	9.45

<sup>a</sup>3.0 equiv of alcohol was used.

and imine 1 were present. Side product aminor 6 (less than 6%) was also observed for 4-cyanoaniline and 4-nitroaniline, confirming the high reactivity of their corresponding imine. It is worthwhile to note neither hemiacetal 5 nor acetal 7 was apparent. All these results are in consistence with the low nucleophilicity of monoalcohols. The equilibrium constants were determined with a range of 0.24–9.45 M<sup>-1</sup>. Albeit small, these equilibrium constants are significantly higher than the data

reported for the reaction of *N*-(*p*-nitrobenzylidene)-*m*-nitroaniline and methanol even in 9:1 methanol/acetonitrile (0.065 M<sup>-1</sup>),<sup>29</sup> thereby further validating the power of our strategy of in situ dynamic multicomponent covalent assembly.

Having achieved imine based DCRs for thiols and alcohols, our next step was to further expand the substrate scope. Compared to dynamic imine formation and exchange with primary amines, DCRs with mono secondary amines are rare.<sup>30</sup> Secondary amines are more sterically hindered than primary amines, and hence less reactive toward nucleophilic addition. The reactivity of primary aromatic amines is also lower than their aliphatic counterparts due to *p*- $\pi$  conjugation. As a result, we postulated that the reactivity of 2 and secondary aliphatic amines would be comparable, and the hemiaminal pathway would be more pronounced. MA was not used for the assembly reaction with diethylamine as a model due to the basicity of aliphatic amines. For the reaction with aniline or 4-methylaniline, only imine was detected (Figure S7). When an EWG was placed on the benzene ring, the peaks of aminorals 4 appeared, and its amount increased with the enhancement of electron-withdrawing ability (Figure S6 and Table 3). The side product (aminor 7) was also

**Table 3. Component Distribution and Equilibrium Constants for Imine 1 Based DCRs with Diethylamine<sup>a</sup>**

X	2-PA (%)	1 (%)	7 (%)	4 (%)	K (M <sup>-1</sup> )
<i>p</i> -Br	<1	93	<1	5	0.40
<i>m</i> -F	3	90	<1	7	0.73
<i>m</i> -Br	3	88	2	7	0.73
<i>m</i> -CF <sub>3</sub>	6	79	3	12	1.41
<i>m</i> -CN	4	76	3	17	1.90
<i>p</i> -CF <sub>3</sub>	7	64	3	26	3.97
<i>p</i> -CN	5	30	3	62	20.4
<i>p</i> -NO <sub>2</sub>	11	13	6	70	57.8

<sup>a</sup>3.0 equiv of diethylamine was used.

detected, but with a smaller percentage than 4, confirming the emergence of the hemiaminal pathway. For 4-cyanoaniline and 4-nitroaniline, 4 was the major component with aminor 7 less than 7%. The equilibrium constant was found with a range of 0.40–57.8 M<sup>-1</sup>.

**LFER Based Correlation.** With a wide range of equilibrium constants available, they were next subjected for linear free energy relationship (LFER) based Hammett analysis to provide insights for further modulation. LFER is one of the most fundamental concepts in chemistry<sup>31</sup> and has been extensively employed to elucidate reaction mechanisms<sup>32</sup> and derive quantitative structure–activity relationships (QSAR).<sup>33</sup> However, the use of LFER for the discovery, modulation, and modeling of thermodynamically driven DCRs is under-explored.<sup>28a</sup> For 1-propanethiol derived assembly, nonlinearity emerged in Hammett plot when the standard Hammett constant  $\sigma$  was employed for the correlation, with *p*-OCH<sub>3</sub> deviating from the line (Figure S17). Instead, a plot of log *K* versus  $\sigma^+$  value of the corresponding substituent afforded a linear relationship with a slope of 1.58 ( $r^2 = 0.987$ , Figure 1a). Analogously, a scattered line was obtained for DCR incorporating diethylamine when  $\sigma$  was used (Figure S18). However, a much stronger linear correlation with  $\sigma^-$  was observed ( $r^2 = 0.989$ , slope = 2.13, Figure 1b), instead of  $\sigma^+$  (Figure S18). A plot of log *K* versus  $\sigma^-$  values also gave a linear relationship for ethanol derived assembly ( $r^2 = 0.986$ , slope = 1.77, Figure 1b), but the correlation with  $\sigma$  or  $\sigma^+$  was poor (Figure S19).

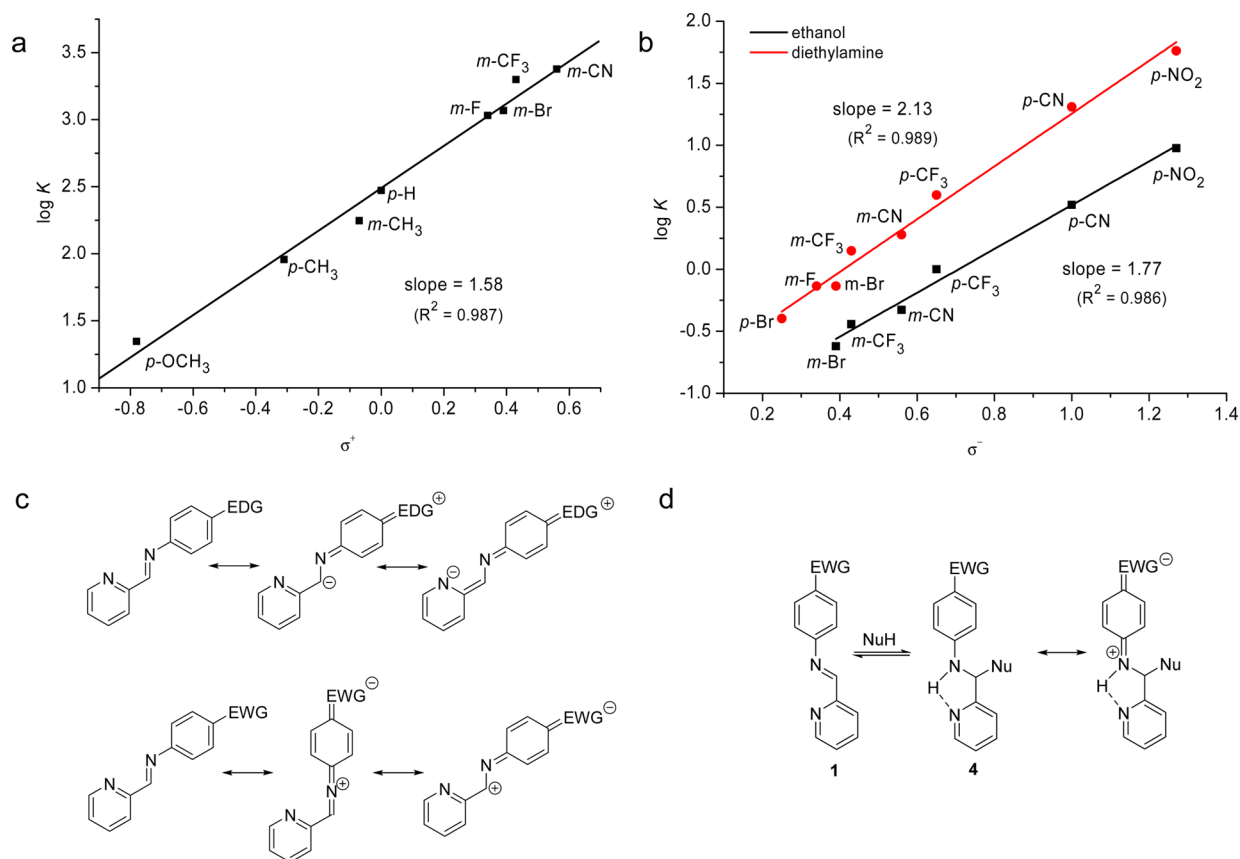


**Figure 1.** LFER based correlation and its rationalization. (a) Hammett plot with  $\sigma^+$  value for the reaction of imine 1 with 1-propanethiol. (b) Hammett plot with  $\sigma^-$  value for the reaction of imine 1 with ethanol and diethylamine, respectively. (c) Resonance effect in imine 1. (d) Resonance stabilization of adduct 4.

The use of different set of Hammett parameter is likely due to the involvement of different stabilizing or activating mechanism.  $\sigma^+$  and  $\sigma^-$  were originally proposed to account for enhanced resonance effects of *para* electron-donating and electron-withdrawing substituents to stabilize positive and negative charges built, respectively, such as those on the benzylic position.<sup>31b</sup> Because our dynamic multicomponent covalent assembly is under thermodynamic control, any resonance effect on the reactant or product can contribute to the  $K$  value. EDGs, such as  $p\text{-OCH}_3$ , stabilize imine 1 via quinoidal resonance, while EWGs exhibit the opposite effect, destabilizing and hence activating the imine (Figure 1c), analogous to our previous report.<sup>28a</sup> For more nucleophilic thiols (larger  $K$  value), the change in  $\log K$  would be more sensitive to the resonance effect in the imine, especially those possessing EDGs. Since resonance stabilization or destabilization takes place in the reactant imine (eq 1), a negative  $\rho$  value would be predicted for the correlation of the dissociation of 4 into imine 1 and thiol with  $\sigma^+$  values. As a result, its reverse reaction, as shown in eq 1, would have a positive  $\rho$  value, in agreement with the experimental data.

Although resonance effects in imine are still valid for the assembly reaction with relatively weak nucleophiles (smaller  $K$  value), such as diethylamine and ethanol, we postulated that the impact resulting from the stabilization of product 4 should be more dominant. One rationalization comes from the enhancement of the acidity of NH by EWGs through quinoidal resonance, thereby increasing the strength of the intramolecular hydrogen bond and stabilizing 4 (Figure 1d). Although partial negative charge is developed on imine nitrogen during the

addition step, difference in thermodynamic stability between imine 1 and adduct 4 must be taken into consideration because equilibrium constants are discussed here, instead of rate constants. From 1 to 4, one N–C bond breaks, and one N–H bond forms (Figure 1d). On the basis of the difference in electronegativity between C (2.55) and H (2.20), the electron density on imine nitrogen increases, and therefore,  $\sigma^-$  is appropriate to correlate the equilibrium from 1 to 4 with a positive  $\rho$  value.

**Unprecedented Nonlinearity with Cyclic Secondary Amines.** Inspired by the finding that different resonance stabilization mode is dominant for DCRs with thiols and secondary amines/alcohols, respectively, we further explored imine based DCRs with cyclic secondary amines, whose nucleophilicity falls generally between thiols and acyclic secondary amines. The multicomponent reactions were conducted with piperidine in the absence of MA (Figure S8), and the distribution of equilibrium mixture is shown in Table 4. No aldehyde was present in all cases. For aniline and its analogues with EDGs, the desired aminal 4 did appear, though the percentage of aminal side product 7 outweighed it. Imines with  $p\text{-OCH}_3$ ,  $p\text{-CH}_3$  or H substitution are rather stable and less reactive (more than 50%), and the creation of aminal 7 is more pronounced than 4. For aniline derivatives bearing EWGs, the amount of imine 1 decreased while product 4 overtook aminal 7. Both 4-cyanoaniline and 4-nitroaniline afforded 4 with a yield more than 70%.

The calculated equilibrium constant for piperidine (1.49–4560  $\text{M}^{-1}$ ) is significantly higher than the corresponding value

**Table 4. Component Distribution and Equilibrium Constants for Imine 1 Based DCRs with Piperidine<sup>a</sup>**

X	1 (%)	7 (%)	4 (%)	K (M <sup>-1</sup> )
<i>p</i> -OCH <sub>3</sub>	82	13	5	1.49
<i>p</i> -CH <sub>3</sub>	69	18	13	6.39
<i>p</i> -H	54	24	22	17.9
<i>m</i> -OCH <sub>3</sub>	52	17	31	27.4
<i>m</i> -Br	36	24	40	107
<i>m</i> -CN	28	20	52	208
<i>p</i> -CF <sub>3</sub>	21	18	61	398
<i>p</i> -CN	13	13	74	883
<i>p</i> -NO <sub>2</sub>	7	8	85	4560

<sup>a</sup>1.1 equiv of piperidine was used.

for diethylamine. For example, with *p*-nitroaniline derived assembly piperidine gave a *K* value (4560 M<sup>-1</sup>) that is 79-fold larger than the *K* value (57.8 M<sup>-1</sup>) for diethylamine. As described in the previous section,  $\sigma^-$  parameters were utilized to correlate the logarithm of *K* values, but the fitting with EDGs was not great (Figure S20). In order to choose the appropriate substituent parameter and thereby rationalize experimental data accordingly, aromatic imines with only *meta* substituents for which quinoidal resonance is impossible were analyzed first, and a straight line was indeed afforded with standard  $\sigma$  values (Figure 2). Placement

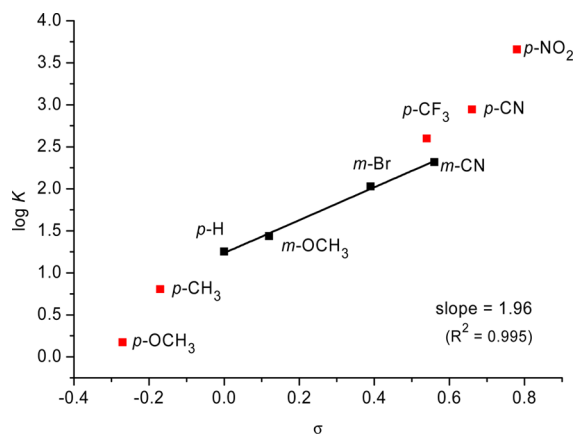


**Figure 2.** Hammett plot with  $\sigma$  value for DCR of imine 1 with piperidine. The linear line was generated by using *K* values from *meta*-substituted aniline and aniline.

of the data from *para* substituents in this plot revealed that both EDGs (*p*-OCH<sub>3</sub> and *p*-CH<sub>3</sub>) and EWGs (*p*-CF<sub>3</sub>, *p*-CN, and *p*-NO<sub>2</sub>) deviate from the line (Figure 2). These results were explained as following: the nucleophilicity of piperidine is between that of 1-propanethiol and diethylamine, and hence, both EDGs and EWGs are able to shift the equilibrium significantly through stabilization of imine 1 and product 4, respectively. As a result, unique nonlinearity emerged in Hammett plot. Such an explanation is also consistent with the trend of equilibrium constants: 1-propanethiol > piperidine > diethylamine.

The nonlinearity in Hammett plot induced by EDGs or EWGs is common in the literature, especially for the kinetics data, and it is generally rationalized as a change in the rate-determining step or reaction mechanism (such as S<sub>N</sub>1 to S<sub>N</sub>2).<sup>34</sup> One notable example is reaction kinetics involving benzylic systems, in which the acceleration of the reaction by both EDGs and EWGs can lead to even “V”- or “U”-shaped Hammett plot.<sup>35</sup> Recently, Um

and co-workers investigated the mechanism of a series of nucleophilic substitution reactions with aromatic esters and revealed that the curved Hammett plot is caused by resonance stabilization of substrates possessing an EDG, instead of a change in the rate-determining step.<sup>36</sup> However, our finding is the first time that both EDGs and EWGs account for the deviation in a thermodynamically driven system, to the best of our knowledge. Correlation with Yukawa-Tsuno equation was also attempted, but similar trend was afforded as the case with  $\sigma^+$  or  $\sigma^-$  alone (Figure S20).

#### Establishment of Unified Reactivity Scales for DCC.

Because different types of substituent parameters were employed for the analysis, the next goal was to develop a set of unified reactivity parameters for DCC. Traditionally, LFER originated reactivity parameters, such as nucleophilicity parameters based on Swain–Scott equation (eq 5)<sup>37</sup> and Brønsted relationship (eq 6),<sup>38</sup> were developed from reaction kinetics and commonly utilized to probe reaction mechanism. Over the past decade, Mayr and co-workers compiled comprehensive reactivity parameter database, and the values of *N* (for nucleophiles) and *E* (for electrophiles) were derived from kinetics data (eq 7).<sup>39</sup> Very recently, they also proposed a quantitative scale of Lewis basicity toward carbocation based Lewis acids (eq 8).<sup>40</sup> Building on the foundation of DCRs involving reactive intermediates, such as iminium ions and their analogues, we recently proposed the concept of reactivity based dynamic covalent chemistry,<sup>26</sup> in which the term “reactivity” describes the extent of the reaction a chemical species participates. It is worthwhile to note that “reactivity” can refer to either reaction equilibrium (thermodynamic reactivity) or rate (kinetic reactivity) depending on circumstances, though traditionally the term is restricted to depict the rate at which a substance tends to undergo a chemical reaction. The use of term “reactivity” in the field of DCC which is under thermodynamic control would unify various DCRs with different functionalities, thus paving the way for the establishment of quantitative scales for DCC.

$$\log(k_{\text{NucX}}/k_{\text{H}_2\text{O}}) = s n_X \quad (5)$$

$$\log k = \beta_{\text{Nuc}} p K_a + \log C' \quad (6)$$

$$\log k = s(N + E) \quad (7)$$

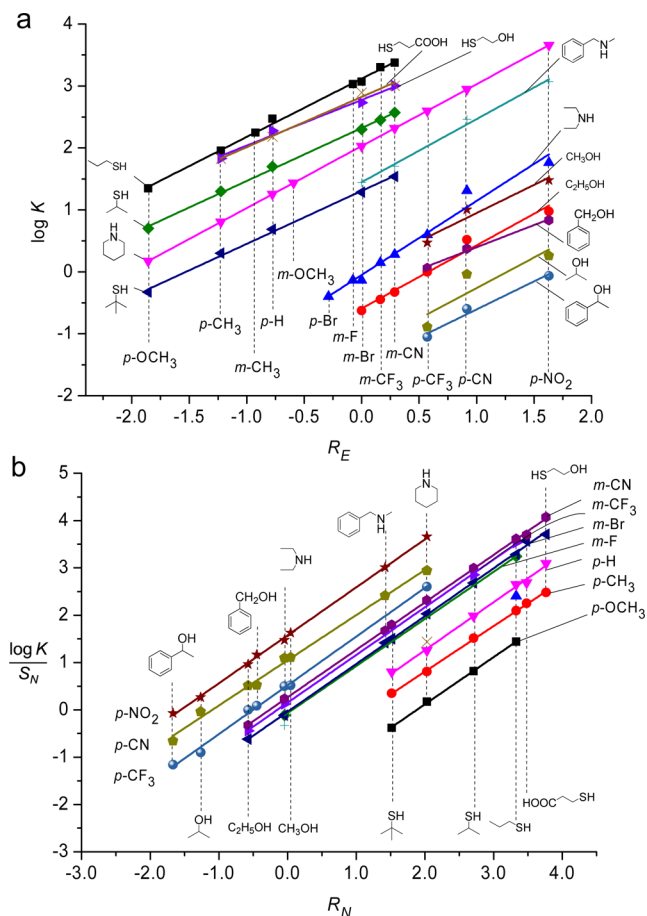
$$\log K = LA + LB \quad (8)$$

$$\log K = S_N(R_N + R_E) \quad (9)$$

$$(\log K)/S_N = R_N + R_E \quad (10)$$

Because most DCRs can be considered as a combination of nucleophiles and electrophiles, we proposed eq 9 to correlate the equilibrium constants, in which *R<sub>N</sub>* is the reactivity parameter for nucleophiles, *R<sub>E</sub>* is the reactivity parameter for electrophiles. *S<sub>N</sub>* is the sensitivity parameter, and its value is nucleophile-specific. In order to expand the substrate scope and hence the generality for the correlation analysis, the dynamic multicomponent covalent assembly reactions were conducted with a set of structurally diverse thiols (1-propanethiol, 2-propanethiol, *t*-butylthiol, 2-mercaptoethanol, and 3-mercaptopropionic acid), secondary amines (diethylamine, *N*-methylbenzylamine, and piperidine), and alcohols (methanol, ethanol, benzyl alcohol, 2-propanol, and 1-phenylethanol) (Figures S9–S14). The corresponding *K* values of DCRs between imine 1 and these mononucleophiles are listed in the Supporting Information, with a broad range of 0.089–4560 M<sup>-1</sup> (Tables S4–S12).

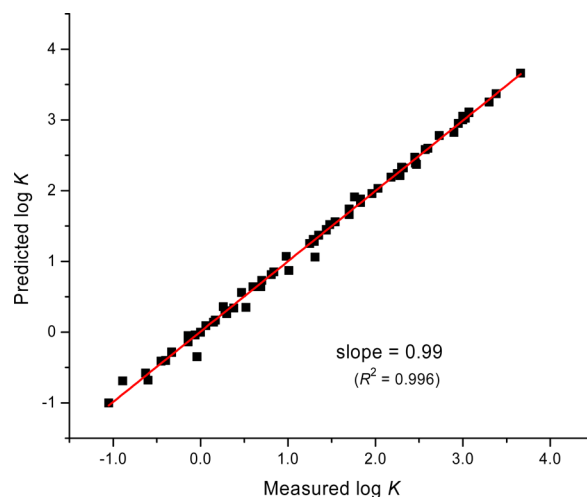
The logarithm of  $K$  values of 66 DCRs were next employed to derive the parameters using the least-squares method on the basis of eq 9 (least-squares minimization of  $\Delta^2 = \sum [\log K - S_N(R_N + R_E)]^2$  by defining  $R_E[\text{I}(m\text{-Br})] = 0$  and  $S_N(\text{piperidine}) = 1$ . Piperidine is chosen due to the availability of equilibrium constants of its reaction with a wide range of imine **1**. High quality of correlations was afforded, as evident in Figure 3a, with



**Figure 3.** Plot of  $\log K$  versus  $R_E$  (a) and plot of  $(\log K)/S_N$  versus  $R_N$  (b) for DCRs of imine **1** with mononucleophiles.

each line corresponding to the DCRs of a certain nucleophile with a series of electrophiles. A range from  $-1.86$  to  $1.63$  was obtained for  $R_E$  while mononucleophiles examined afforded an  $R_N$  range from  $-1.67$  to  $3.76$  and an  $S_N$  range from  $0.72$  to  $1.20$ , respectively. In another way of illustrating the reactivity parameters proposed, the plot of  $(\log K)/S_N$  versus  $R_N$  was linear with a slope equal or close to 1 (eq 10), in which each line refers to the DCRs of a certain electrophile with a series of nucleophiles (Figure 3b). Although plots in Figure 3a and 3b are mathematically equivalent (eq 9 and 10), the correlation of  $(\log K)/S_N$  as a function of  $R_N$  is important because it can be used to deduce  $R_E$  value of electrophiles from their DCRs with a set of nucleophiles whose  $R_N$  and  $S_N$  values are known (see details below).

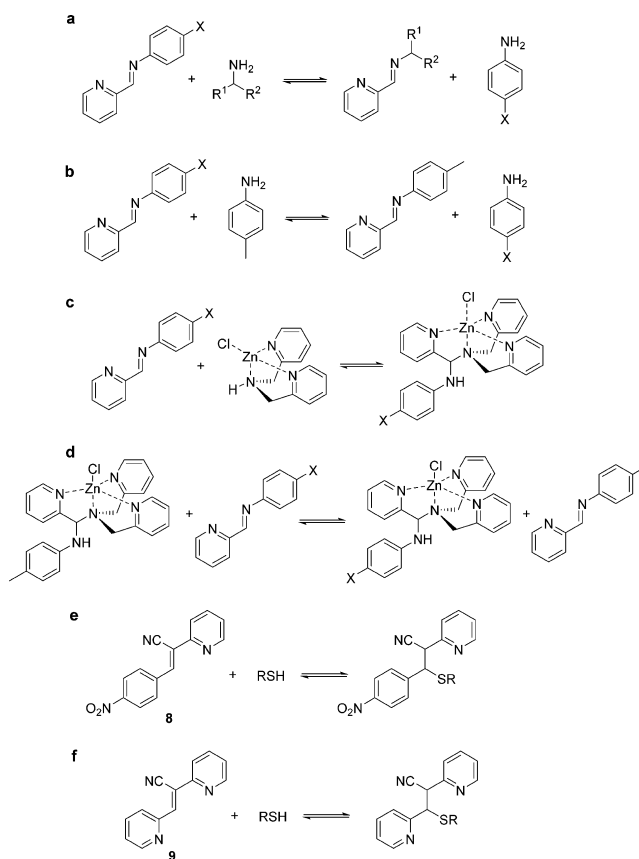
To verify the overall quality as well as predictive capability of the correlation, the  $\log K$  values of 66 DCRs predicted using eq 9 were plotted as a function of the measured  $\log K$  values. An excellent linear relationship was afforded ( $R^2 = 0.996$ , slope =  $0.99$ , Figure 4), thus further validating the effectiveness of our model.



**Figure 4.** Linear correlation of  $\log K$  values predicted using eq 9 with the measured  $\log K$  values (66 DCRs).

**Application of the Reactivity Scales for DCC.** Having established quantitative reactivity scales with reference DCRs, we next set out to further examine their application scope and predictive ability. First, an approach for the correlation with primary aliphatic amines was developed. Due to their high nucleophilicity, we postulated that a dynamic component exchange reaction of amines would be plausible (Scheme 2a). To test this hypothesis, a one pot dynamic multicomponent reaction of **2-PA**, 1-butylamine, and aromatic amine **2** was

**Scheme 2.** Application of the Reactivity Scales for Other DCRs



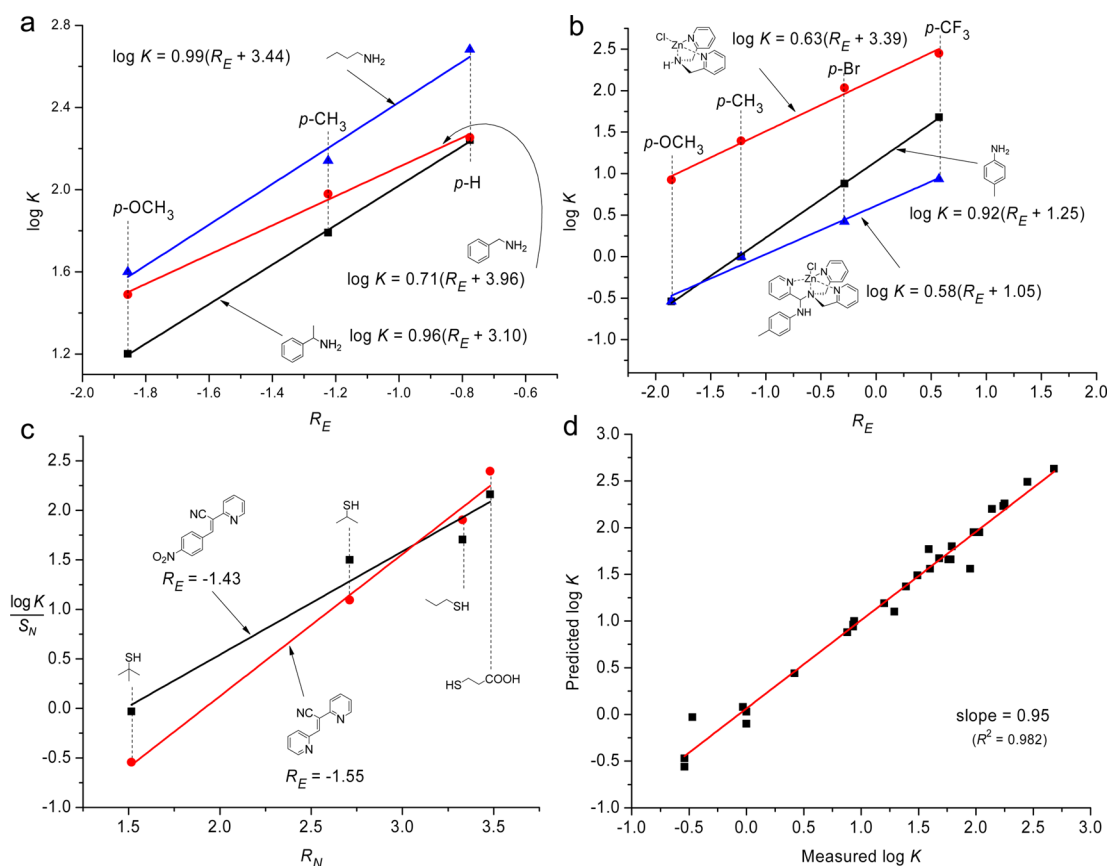


**Figure 5.** Correlation of DCRs in Scheme 2 with reactivity parameters established. (a) Imine based DCRs with primary aliphatic amines (Scheme 2a). (b) Imine based DCRs with primary aromatic amines (Scheme 2b) and metal complexes (Scheme 2c and 2d). (c) DCRs between Michael acceptors and thiols (Scheme 2e and 2f). (d) Linear correlation of  $\log K$  values predicted using eq 9 with the measured  $\log K$  values for DCRs in Scheme 2 (29 reactions).

performed.  $^1\text{H NMR}$  revealed the presence of both imines, and the  $K$  value for the amine exchange reaction was calculated (Tables S13–S15). With a series of substituted imine **1**, the correlation of  $\log K$  with the corresponding  $R_E$  values gave an  $R_N$  value of 3.44 for 1-butylamine (Figure 5a). Analogous analysis was also conducted with benzylamine and  $\alpha$ -methylbenzylamine, and they have an  $R_N$  value of 3.96 and 3.10, respectively.

The  $R_E$  values were next utilized to correlate other DCRs we developed recently.<sup>28a</sup> The equilibrium reaction of imine **1** and zinc complex of di(2-picolyl)amine ( $\text{Zn}^{2+}$ -DPA) to create tripodal metal complexes as well as its associated dynamic component exchange (Figure 5b–d) was hence subjected for analysis using eq 9. As shown in Figure 5b, a straight line as a function of  $R_E$  was afforded for all three DCRs, indicative of the versatility of the developed reactivity parameters. Furthermore, the  $R_N$  value of 4-methylaniline was found to be 1.25 based on the correlation of  $\log K = 0.92(1.25 + R_E)$ . Alternatively, the reverse reaction of the imine/amine exchange in Scheme 2b was employed to predict the  $R_N$  values of aromatic amines in conjunction with the  $R_E$  values of **1** ( $p\text{-CH}_3$ ). The following eq 9 was employed:  $\log K = 0.92\{R_N + R_E [1(p\text{-CH}_3)]\}$  (the  $K$  value is for the reverse reaction of Scheme 2b; assuming that same  $S_N$  value for aromatic amines examined here). The  $R_N$  value for  $p\text{-OMe}$ ,  $p\text{-Me}$ ,  $p\text{-Br}$ , and  $p\text{-CF}_3$  substituted aniline was estimated to be 1.81, 1.22, 0.26, and  $-0.60$ , respectively. The  $R_N$  value for 4-methylaniline (1.22) is in close agreement with the data (1.25) obtained from the correlation in Figure 5b. As a result, the DCRs of aromatic imines enabled us to develop reactivity parameters

for thiols, primary amines, secondary amines, and alcohols, which are widespread in chemistry and are among the most used functionalities in dynamic covalent and systems chemistry.

To further prove the generality of reactivity scales described herein, other class of electrophiles was investigated. Toward this end, dynamic thio-Michael reactions of  $\alpha$ -[(4-nitrophenyl)methylene]-2-pyridineacetonitrile (**8**) and  $\alpha$ -(2-pyridinylmethylene)-2-pyridineacetonitrile (**9**) were employed, respectively (Scheme 2e and 2f). These DCRs have application potential in biology as analogous DCRs have been used for the reversible covalent targeting of cysteine residues in protein kinases.<sup>19</sup> A quantitative reactivity scale would facilitate the design and optimization of potential DCRs. The reactions with a series of monothiols were conducted first in  $\text{CD}_3\text{CN}$  (Figures S15 and S16). A linear relationship of  $(\log K)/S_N$  with  $R_N$  values was afforded, though the slope was found to be 1.04 and 1.44 for **8** and **9**, respectively. By using the least-squares method and fixing the slope for the correlation of  $(\log K)/S_N$  versus  $R_N$  to one as required by eq 10, an  $R_E$  value of  $-1.43$  and  $-1.55$  was found for **8** and **9** in acetonitrile, respectively (Figure 5c). The DCRs were also conducted in DMSO, and larger  $K$  values were found (Table S37). The plot of  $(\log K)/S_N$  versus  $R_N$  afforded modest quality of fitting (Table S37). This is because different reactivity parameters would be expected in DMSO. Nevertheless, the application of reactivity scales in different solvents further validates the generality of our approach. Again, a linear correlation between predicted  $\log K$  values and measured  $\log K$  values was found for DCRs listed in Scheme 2 ( $R^2 = 0.982$ ,

slope = 0.95, Figure Sd). Moreover, we expect no hurdle to expanding the scales to other types of DCRs and functionalities.

## CONCLUSIONS

In summary, quantitative reactivity scales were developed for dynamic covalent chemistry based upon universal dynamic covalent reactions between aromatic imines and a series of mononucleophiles. The dynamic multicomponent covalent assembly was conducted to generate imine in situ and control the equilibrium. The reactions were fine-tuned through substituent effect, and the equilibrium constants were examined through Hammett analysis. It is found that both the set of the Hammett parameter as well as the sensitivity to substitution are dependent on the nucleophilicity of the substrate. EDGs stabilize the imine through quinonoidal resonance, while EWGs stabilize the product by enhancing intramolecular hydrogen bonding. For DCRs with cyclic secondary amines, unique nonlinearity induced by both EDGs and EWGs emerged in Hammett plot. Quantitative physical organic scales for DCC were then developed by establishing unified reactivity parameters with imine based DCRs as references, and the  $R_N$  and  $S_N$  values for a series of structurally diverse O-, N-, and S- mononucleophiles were obtained (Figure 6). The correlation with other DCRs was

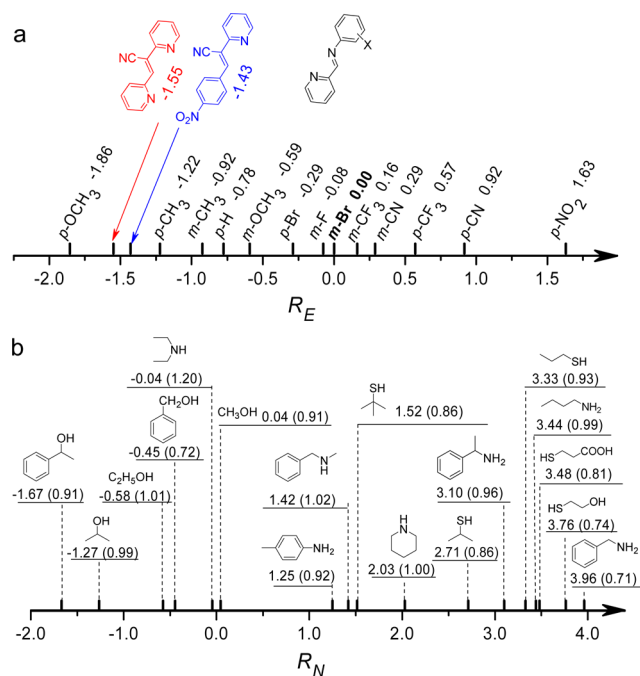


**Figure 6.** Summary of the quantitative scale of  $R_E$  (a) and  $R_N$  (b). The associated  $S_N$  value for  $R_N$  is in the parentheses.

also achieved, thus demonstrating the generality and predictive power of our approach. The concept of reactivity based DCRs should be applicable to other reversible systems, and the compilation of comprehensive reactivity scales for DCC is currently underway.

## ASSOCIATED CONTENT

### Supporting Information

The Supporting Information is available free of charge on the ACS Publications website at DOI: 10.1021/jacs.5b11361.

Experimental procedures, characterization, selected NMR spectra, component distribution at equilibrium, additional LFER analysis, and data for correlation analysis. (PDF)

## AUTHOR INFORMATION

### Corresponding Author

\*lyou@fjirsm.ac.cn

### Author Contributions

<sup>§</sup>Y.Z., L.L., and H.Y. contributed equally.

### Notes

The authors declare no competing financial interest.

## ACKNOWLEDGMENTS

We thank The Recruitment Program of Global Youth Experts, National Natural Science Foundation of China (21403239), and National Science Foundation of Fujian Province, China (2014J05024) for financial support. We also thank The CAS/SAFEA International Partnership Program for Creative Research Teams.

## REFERENCES

- (1) (a) Herrmann, A. *Chem. Soc. Rev.* **2014**, *43*, 1899–1933. (b) Jin, Y.; Yu, C.; Denman, R. J.; Zhang, W. *Chem. Soc. Rev.* **2013**, *42*, 6634–6654. (c) Lehn, J.-M. *Chem. Soc. Rev.* **2007**, *36*, 151–160. (d) Corbett, P. T.; Leclaire, J.; Vial, L.; West, K. R.; Wietor, J.-L.; Sanders, J. K.; Otto, S. *Chem. Rev.* **2006**, *106*, 3652–3711. (e) Rowan, S. J.; Cantrell, S. J.; Cousins, G. R. L.; Sanders, J. K. M.; Stoddart, J. F. *Angew. Chem., Int. Ed.* **2002**, *41*, 898–952.
- (2) (a) Wilson, A.; Gasparini, G.; Matile, S. *Chem. Soc. Rev.* **2014**, *43*, 1948–1962. (b) Jin, Y.; Wang, Q.; Taynton, P.; Zhang, W. *Acc. Chem. Res.* **2014**, *47*, 1575–1586. (c) Moulin, E.; Cormos, G.; Giuseppone, N. *Chem. Soc. Rev.* **2012**, *41*, 1031–1049.
- (3) (a) Huang, Y.-J.; Ouyang, W.-J.; Wu, X.; Li, Z.; Fossey, J. S.; James, T. D.; Jiang, Y.-B. *J. Am. Chem. Soc.* **2013**, *135*, 1700–1703. (b) You, L.; Zha, D.; Anslyn, E. V. *Chem. Rev.* **2015**, *115*, 7840–7892. (c) James, L. L.; Beaver, J. E.; Rice, N. W.; Waters, M. L. *J. Am. Chem. Soc.* **2013**, *135*, 6450–6455.
- (4) (a) Boutoureira, O.; Bernardes, G. J. L. *Chem. Rev.* **2015**, *115*, 2174–2195. (b) Tomás-Gamasa, M.; Serdjukow, S.; Su, M.; Müller, M.; Carell, T. *Angew. Chem., Int. Ed.* **2015**, *54*, 796–800. (c) Gamboa Varela, J.; Gates, K. S. *Angew. Chem., Int. Ed.* **2015**, *54*, 7666–7669. (d) Price, N. E.; Johnson, K. M.; Wang, J.; Fekry, M. I.; Wang, Y.; Gates, K. S. *J. Am. Chem. Soc.* **2014**, *136*, 3483–3490.
- (5) (a) Schaufelberger, F.; Ramström, O. *Chem. - Eur. J.* **2015**, *21*, 12735–12740. (b) Dydio, P.; Breuil, P.-A. R.; Reek, J. N. H. *Isr. J. Chem.* **2013**, *53*, 61–74. (c) Gasparini, G.; Dal Molin, M.; Prins, L. *J. Org. Chem.* **2010**, *2010*, 2429–2440.
- (6) (a) Hsu, C.-W.; Miljanić, O. Š. *Angew. Chem., Int. Ed.* **2015**, *54*, 2219–2222. (b) Hafezi, N.; Lehn, J.-M. *J. Am. Chem. Soc.* **2012**, *134*, 12861–12868. (c) Osowska, K.; Miljanić, O. Š. *Angew. Chem., Int. Ed.* **2011**, *50*, 8345–8349.
- (7) (a) Ruiz-Mirazo, K.; Briones, C.; de la Escosura, A. *Chem. Rev.* **2014**, *114*, 285–366. (b) Grzybowski, B.; Otto, S.; Philp, D. *Chem. Commun.* **2014**, *50*, 14924–14925. (c) Li, J.; Nowak, P.; Otto, S. *J. Am. Chem. Soc.* **2013**, *135*, 9222–9239. (d) Giuseppone, N. *Acc. Chem. Res.* **2012**, *45*, 2178–2188.
- (8) (a) Nowak, P.; Colomb-Delsuc, M.; Otto, S.; Li, J. *J. Am. Chem. Soc.* **2015**, *137*, 10965–10969. (b) McGonigal, P. R.; Stoddart, J. F. *Nat. Chem.* **2013**, *5*, 260–262. (c) Ponnuswamy, N.; Coughon, F. B. L.; Clough, J. M.; Pantoş, G. D.; Sanders, J. K. M. *Science* **2012**, *338*, 783–785. (d) Ayme, J.-F.; Beves, J. E.; Leigh, D. A.; McBurney, R. T.; Rissanen, K.; Schultz, D. *Nat. Chem.* **2012**, *4*, 15–20.
- (9) (a) Wood, D. M.; Meng, W.; Ronson, T. K.; Stefankiewicz, A. R.; Sanders, J. K. M.; Nitschke, J. R. *Angew. Chem., Int. Ed.* **2015**, *54*, 3988–3992. (b) Ayme, J.-F.; Beves, J. E.; Campbell, C. J.; Gil-Ramírez, G.; Leigh, D. A.; Stephens, A. J. *J. Am. Chem. Soc.* **2015**, *137*, 9812–9815.



- (c) Campbell, C. J.; Leigh, D. A.; Vitorica-Yrezabal, I. J.; Woltering, S. L. *Angew. Chem., Int. Ed.* **2014**, *53*, 13771–13774. (d) Ronson, T. K.; League, A. B.; Gagliardi, L.; Cramer, C. J.; Nitschke, J. R. *J. Am. Chem. Soc.* **2014**, *136*, 15615–15624. (e) Ayme, J.-F.; Beves, J. E.; Campbell, C. J.; Leigh, D. A. *Chem. Soc. Rev.* **2013**, *42*, 1700–1712. (f) Campbell, V. E.; de Hatten, X.; Delsuc, N.; Kauffmann, B.; Huc, I.; Nitschke, J. R. *Nat. Chem.* **2010**, *2*, 684–687.
- (10) della Sala, F.; Kay, E. R. *Angew. Chem., Int. Ed.* **2015**, *54*, 4187–4191.
- (11) (a) Kovaříček, P.; Lehn, J.-M. *Chem. - Eur. J.* **2015**, *21*, 9380–9384. (b) Kovaříček, P.; Lehn, J.-M. *J. Am. Chem. Soc.* **2012**, *134*, 9446–9455.
- (12) (a) Mastalerz, M.; Schneider, M. W.; Opper, I. M.; Presly, O. *Angew. Chem., Int. Ed.* **2011**, *50*, 1046–1051. (b) Uribe-Romo, F. J.; Doonan, C. J.; Furukawa, H.; Oisaki, K.; Yaghi, O. M. *J. Am. Chem. Soc.* **2011**, *133*, 11478–11481. (c) Zhang, G.; Mastalerz, M. *Chem. Soc. Rev.* **2014**, *43*, 1934–1947. (d) Zhang, G.; Presly, O.; White, F.; Opper, I. M.; Mastalerz, M. *Angew. Chem., Int. Ed.* **2014**, *53*, 1516–1520. (e) Sakaushi, K.; Antonietti, M. *Acc. Chem. Res.* **2015**, *48*, 1591–1600. (f) Zeng, Y.; Zou, R.; Luo, Z.; Zhang, H.; Yao, X.; Ma, X.; Zou, R.; Zhao, Y. *J. Am. Chem. Soc.* **2015**, *137*, 1020–1023.
- (13) Gasparini, G.; Dal Molin, M.; Lovato, A.; Prins, L. J. In *Supramolecular Chemistry*; John Wiley & Sons, Ltd, 2012.
- (14) (a) Belowich, M. E.; Stoddart, J. F. *Chem. Soc. Rev.* **2012**, *41*, 2003–2024. (b) Herrmann, A. *Org. Biomol. Chem.* **2009**, *7*, 3195–3204. (c) Meyer, C. D.; Joiner, C. S.; Stoddart, J. F. *Chem. Soc. Rev.* **2007**, *36*, 1705–1723. (d) Jia, Y.; Li, J. *Chem. Rev.* **2015**, *115*, 1597–1621.
- (15) (a) Tatum, L. A.; Su, X.; Aprahamian, I. *Acc. Chem. Res.* **2014**, *47*, 2141–2149. (b) Beeren, S. R.; Pittelkow, M.; Sanders, J. K. *Chem. Commun.* **2011**, *47*, 7359–7361.
- (16) Black, S. P.; Sanders, J. K. M.; Stefankiewicz, A. R. *Chem. Soc. Rev.* **2014**, *43*, 1861–1872.
- (17) (a) Sun, X.; James, T. D. *Chem. Rev.* **2015**, *115*, 8001–8037. (b) Bull, S. D.; Davidson, M. G.; van den Elsen, J. M. H.; Fossey, J. S.; Jenkins, A. T. A.; Jiang, Y.-B.; Kubo, Y.; Marken, F.; Sakurai, K.; Zhao, J.; James, T. D. *Acc. Chem. Res.* **2013**, *46*, 312–326.
- (18) (a) Lu, G.; Yang, H.; Zhu, Y.; Huggins, T.; Ren, Z. J.; Liu, Z.; Zhang, W. *J. Mater. Chem. A* **2015**, *3*, 4954–4959. (b) Wang, Q.; Yu, C.; Long, H.; Du, Y.; Jin, Y.; Zhang, W. *Angew. Chem., Int. Ed.* **2015**, *54*, 7550–7554. (c) Yang, H.; Du, Y.; Wan, S.; Trahan, G. D.; Jin, Y.; Zhang, W. *Chem. Sci.* **2015**, *6*, 4049–4053.
- (19) (a) Bradshaw, J. M.; McFarland, J. M.; Paavilainen, V. O.; Bisconte, A.; Tam, D.; Phan, V. T.; Romanov, S.; Finkle, D.; Shu, J.; Patel, V.; Ton, T.; Li, X.; Loughhead, D. G.; Nunn, P. A.; Karr, D. E.; Gerritsen, M. E.; Funk, J. O.; Owens, T. D.; Verner, E.; Brameld, K. A.; Hill, R. J.; Goldstein, D. M.; Taunton, J. *Nat. Chem. Biol.* **2015**, *11*, 525–531. (b) Krishnan, S.; Miller, R. M.; Tian, B.; Mullins, R. D.; Jacobson, M. P.; Taunton, J. *J. Am. Chem. Soc.* **2014**, *136*, 12624–12630. (c) Miller, R. M.; Paavilainen, V. O.; Krishnan, S.; Serafimova, I. M.; Taunton, J. *J. Am. Chem. Soc.* **2013**, *135*, 5298–5301. (d) Joshi, G.; Anslyn, E. V. *Org. Lett.* **2012**, *14*, 4714–4717. (e) Serafimova, I. M.; Pufall, M. A.; Krishnan, S.; Duda, K.; Cohen, M. S.; Maglathlin, R. L.; McFarland, J. M.; Miller, R. M.; Frödin, M.; Taunton, J. *Nat. Chem. Biol.* **2012**, *8*, 471–476.
- (20) (a) Brachvogel, R.-C.; von Delius, M. *Chem. Sci.* **2015**, *6*, 1399–1403. (b) Brachvogel, R.-C.; Hampel, F.; von Delius, M. *Nat. Commun.* **2015**, *6*, 7129.
- (21) Sanchez-Sanchez, A.; Fulton, D. A.; Pomposo, J. A. *Chem. Commun.* **2014**, *50*, 1871–1874.
- (22) (a) Larsen, D.; Pittelkow, M.; Karmakar, S.; Kool, E. T. *Org. Lett.* **2015**, *17*, 274–277. (b) Sato, T.; Amamoto, Y.; Yamaguchi, H.; Ohishi, T.; Takahara, A.; Otsuka, H. *Polym. Chem.* **2012**, *3*, 3077–3083.
- (23) (a) Ji, S.; Cao, W.; Yu, Y.; Xu, H. *Angew. Chem., Int. Ed.* **2014**, *53*, 6781–6785. (b) Rasmussen, B.; Sørensen, A.; Gotfredsen, H.; Pittelkow, M. *Chem. Commun.* **2014**, *50*, 3716–3718. (c) Zhang, S.; Wang, X.; Su, Y.; Qiu, Y.; Zhang, Z.; Wang, X. *Nat. Commun.* **2014**, *5*, 4127. (d) Ren, H.; Huang, Z.; Yang, H.; Xu, H.; Zhang, X. *ChemPhysChem* **2015**, *16*, 523–527.
- (24) (a) Røling, O.; De Bruycker, K.; Vonhören, B.; Stricker, L.; Körsgen, M.; Arlinghaus, H. F.; Ravoo, B. J.; Du Prez, F. E. *Angew. Chem., Int. Ed.* **2015**, *54*, 13126–13129. (b) Billiet, S.; De Bruycker, K.; Driessen, F.; Goossens, H.; Van Speybroeck, V.; Winne, J. M.; Du Prez, F. E. *Nat. Chem.* **2014**, *6*, 815–821.
- (25) Delebecq, E.; Pascual, J.-P.; Boutevin, B.; Ganachaud, F. *Chem. Rev.* **2013**, *113*, 80–118.
- (26) (a) Zhou, Y.; Ye, H.; You, L. *J. Org. Chem.* **2015**, *80*, 2627–2633. (b) Ren, Y.; You, L. *J. Am. Chem. Soc.* **2015**, *137*, 14220–14228.
- (27) (a) Layer, R. W. *Chem. Rev.* **1963**, *63*, 489–510. (b) Arrayas, R. G.; Carretero, J. C. *Chem. Soc. Rev.* **2009**, *38*, 1940–1948. (c) Xie, J.-H.; Zhu, S.-F.; Zhou, Q.-L. *Chem. Rev.* **2011**, *111*, 1713–1760. (d) Kobayashi, S.; Mori, Y.; Fossey, J. S.; Salter, M. M. *Chem. Rev.* **2011**, *111*, 2626–2704. (e) Waser, M.; Novacek, J. *Angew. Chem., Int. Ed.* **2015**, *54*, 14228–14231. (f) Wu, Y.; Hu, L.; Li, Z.; Deng, L. *Nature* **2015**, *523*, 445–450.
- (28) (a) Zhou, Y.; Yuan, Y.; You, L.; Anslyn, E. V. *Chem. - Eur. J.* **2015**, *21*, 8207–8213. (b) Schaufelberger, F.; Hu, L.; Ramström, O. *Chem. - Eur. J.* **2015**, *21*, 9776–9783. (c) Biondi, M.; Pilati, S.; Cacciapaglia, R.; Mandolini, L.; Di Stefano, S. *Org. Biomol. Chem.* **2014**, *12*, 3282–3287.
- (29) Ogata, Y.; Kawasaki, A. *J. Org. Chem.* **1974**, *39*, 1058–1061.
- (30) (a) Körsten, S.; Mohr, G. *J. Chem. - Eur. J.* **2011**, *17*, 969–975. (b) Godin, G.; Levrant, B.; Trachsel, A.; Lehn, J.-M.; Herrmann, A. *Chem. Commun.* **2010**, *46*, 3125–3127.
- (31) (a) Jaffé, H. H. *Chem. Rev.* **1953**, *53*, 191–261. (b) Hansch, C.; Leo, A.; Taft, R. W. *Chem. Rev.* **1991**, *91*, 165–195.
- (32) (a) Bour, J. R.; Camasso, N. M.; Sanford, M. S. *J. Am. Chem. Soc.* **2015**, *137*, 8034–8037. (b) Pulkukody, R.; Kyran, S. J.; Drummond, M. J.; Hsieh, C.-H.; Darensbourg, D. J.; Darensbourg, M. Y. *Chem. Sci.* **2014**, *5*, 3795–3802. (c) He, C.; Ke, J.; Xu, H.; Lei, A. *Angew. Chem., Int. Ed.* **2013**, *52*, 1527–1530. (d) Mueller, J. A.; Sigman, M. S. *J. Am. Chem. Soc.* **2003**, *125*, 7005–7013. (e) Böhm, V. P. W.; Herrmann, W. A. *Chem. - Eur. J.* **2001**, *7*, 4191–4197.
- (33) (a) Hansch, C.; Hoekman, D.; Leo, A.; Weininger, D.; Selassie, C. D. *Chem. Rev.* **2002**, *102*, 783–812. (b) Hansch, C. *Acc. Chem. Res.* **1969**, *2*, 232–239.
- (34) (a) McGrath, J. M.; Pluth, M. D. *J. Org. Chem.* **2014**, *79*, 11797–11801. (b) Huang, Y.; Wayner, D. D. M. *J. Am. Chem. Soc.* **1994**, *116*, 2157–2158. (c) Kandamarachchi, P.; Sinnott, M. L. *J. Am. Chem. Soc.* **1994**, *116*, 5592–5600.
- (35) (a) Young, P. R.; Jencks, W. P. *J. Am. Chem. Soc.* **1979**, *101*, 3288–3294. (b) Stein, A. R.; Tencer, M.; Moffatt, E. A.; Dawe, R.; Sweet, J. J. *Org. Chem.* **1980**, *45*, 3539–3540. (c) Richard, J. P.; Jencks, W. P. *J. Am. Chem. Soc.* **1982**, *104*, 4689–4691.
- (36) (a) Um, I.-H.; Bae, A.-R.; Um, T.-I. *J. Org. Chem.* **2014**, *79*, 1206–1212. (b) Um, I.-H.; Bae, A. R. *J. Org. Chem.* **2012**, *77*, 5781–5787. (c) Um, I.-H.; Bae, A. R. *J. Org. Chem.* **2011**, *76*, 7510–7515.
- (37) (a) Swain, C. G.; Scott, C. B. *J. Am. Chem. Soc.* **1953**, *75*, 141–147. (b) Pearson, R. G.; Sobel, H. R.; Songstad, J. J. *J. Am. Chem. Soc.* **1968**, *90*, 319–326.
- (38) (a) Bender, M. L. *Chem. Rev.* **1960**, *60*, 53–113. (b) Lewis, E. S. *J. Phys. Org. Chem.* **1990**, *3*, 1–8.
- (39) (a) Mayr, H. *Tetrahedron* **2015**, *71*, 5095–5111. (b) Guo, X.; Mayr, H. *J. Am. Chem. Soc.* **2014**, *136*, 11499–11512. (c) Appel, R.; Chelli, S.; Tokuyasu, T.; Troshin, K.; Mayr, H. *J. Am. Chem. Soc.* **2013**, *135*, 6579–6587. (d) Appel, R.; Mayr, H. *J. Am. Chem. Soc.* **2011**, *133*, 8240–8251. (e) Mayr, H.; Kempf, B.; Ofial, A. R. *Acc. Chem. Res.* **2003**, *36*, 66–77. (f) Mayr, H.; Bug, T.; Gotta, M. F.; Hering, N.; Irrgang, B.; Janker, B.; Kempf, B.; Loos, R.; Ofial, A. R.; Remennikov, G.; Schimmel, H. *J. Am. Chem. Soc.* **2001**, *123*, 9500–9512. (g) Mayr, H.; Patz, M. *Angew. Chem., Int. Ed. Engl.* **1994**, *33*, 938–957.
- (40) Mayr, H.; Ammer, J.; Baidya, M.; Maji, B.; Nigst, T. A.; Ofial, A. R.; Singer, T. *J. Am. Chem. Soc.* **2015**, *137*, 2580–2599.